

## KINEMATIC ANALYSIS OF AUTOMOTIVE SUSPENSIONS USING DAVIES' METHOD

**Jorge Luiz Erthal, jlerthal@utfpr.edu.br**

Universidade Tecnológica Federal do Paraná

**Lauro Cesar Nicolazzi, lauro@grante.ufsc.br**

**Daniel Martins, daniel@emc.ufsc.br**

Universidade Federal de Santa Catarina

**Abstract.** *This article presents a mathematical model for kinematic analysis of vehicle suspensions using Davies' method and Assur virtual chains. Davies' method considers two forms of obtaining kinematic equations: by Kirchhoff's Circuit Law and by Virtual Power. The kinematic chain is represented by graphs. Using Circuit Law, kinematic equations are established between links belonging to each circuit of the kinematic chain. An Assur virtual chain is used for positioning the chassis. The presented model is planar, has two degrees-of-freedom, and is composed by a chassis and two sets of McPherson-type independent suspensions. The model provides roll center, tread width and camber for each position and orientation of the chassis. The model also provides a systematic way to obtain the relative movements between any pair of components.*

**Keywords:** *Davies' method, automotive suspension, kinematics, virtual power, screw theory*

### 1. INTRODUCTION

There are several approaches to model vehicle dynamics representing vertical, longitudinal and lateral behavior. Vertical dynamics analysis normally uses half and quarter car models (Gillespie, 1992). Longitudinal dynamics uses the longitudinal static model in order to predict driving and braking performances (Gillespie, 1992; Dixon, 1996; Rill, 2003). Lateral dynamics analysis uses planar models with two or four wheels in order to evaluate steering system, cornering forces, steady state handling, rollover threshold and load transfers (Gillespie, 1992; Dixon, 1996; Reimpell et al., 2001; Rill, 2003). These models normally present simplifications on suspension representation *e.g.* in the rollover models (Gillespie, 1992; Hac, 2002). Including links and joints properties it is possible to represent the influence of the suspension parameters (camber, toe, caster) in the dynamic behavior of the vehicle (Chen and Beale, 2003; Mántaras et al., 2004).

The use of computational techniques to derive and solve constitutive equations which describe the behavior of the system is a current practice. Using multi-body based softwares, suspensions can be modeled with more details including external forces and prescribed motion (Costa Neto, 1992; Perna et al., 2000; Shabana, 2003; Chang and Joo, 2005). However sometimes it is possible to improve the representation of the simplified model avoiding the use of more complex and expensive techniques. In this context, this article presents a suspension planar model based on Davies' method and Assur kinematic chains. Such model can represent the rollover behavior of a vehicle and allows to get information not supplied for similar models.

Davies' method uses screw theory and graph theory together with Kirchhoff laws for build and to solve mechanisms kinematics and statics in a concise and compact way (Davies, 2000; Campos et al., 2005). The method can be used in vehicle modeling, particularly in such mechanical systems as suspensions and steering systems, due to the easiness of to settle down and to solve relationships between motion (twists) and action (wrenches).

A motion screw or *twist* ( $\$$ ) is a dual vector that represents the displacement of a rigid body as a combination of translation along a *screw axis* and rotation about the same axis (Gallardo et al., 2003). A twist has the form

$$\$ = \begin{Bmatrix} \omega \\ v_O \end{Bmatrix} \quad (1)$$

where  $\omega$  is the angular velocity of the considered body and  $v_O$  is the velocity of the body point that is coincident with point  $O$ , the origin of the reference system. A twist may be decomposed into its magnitude,  $\varphi$ , and its corresponding normalized screw,  $\hat{\$}$ , *i.e.*

$$\$ = \hat{\$} \cdot \varphi = \begin{Bmatrix} s \\ s_O \times s + \lambda s \end{Bmatrix} = \{ r \ s \ t \ u \ v \ w \}^T, \quad (2)$$

where  $s$  is a unit vector pointing along the direction of the screw axis,  $s_O$  is the position vector of any point on the screw axis, and  $\lambda$  is the *pitch* (Tsai, 1999). For *revolute* and *prismatic* pairs, twists are represented, respectively, by

$$\hat{\$} = \begin{Bmatrix} s \\ s_O \times s \end{Bmatrix} \quad \text{and} \quad \hat{\$} = \begin{Bmatrix} 0 \\ s \end{Bmatrix}. \quad (3)$$

Screw theory has been applied mainly in problems related to differential kinematic and statics of serial and parallel robotic manipulators (Tsai, 1998; Tsai, 1999; Valdiero et al., 2001; Campos et al., 2003), including analysis of redundancy (Campos et al., 2003) and of singularities (Tsai, 1998; Martins, 2002). Fundamentals and applications on screw theory can be found in (Hunt, 1978; Davies, 1995a; Tsai, 1999; Davidson and Hunt, 2004).

The other tool used in Davies' method is the graph theory. A graph consists of a set of vertex connected by a set of edges. When a graph represents a kinematic chain, the vertex represent the bodies and the edges represent the couples or their movements. Graph theory can be found in (Davies, 1995b; Tsai, 2000; Fayet, 2000).

Besides Davies' Method, the proposed model uses the concept of Assur virtual chain. An Assur virtual chain is a kinematic chain composed of virtual links and virtual joints satisfying the following three properties: a) the virtual chain is open; b) it has joints whose normalized screws are linearly independent; and c) it does not change the mobility of the real kinematic chain (Campos et al., 2005). Using Assur virtual kinematic chain is possible to obtain information about the movement of a kinematic chain or to impose movements on a kinematic chain. A systematic method for calculation of the differential kinematics of manipulators an extension of Davies method, using the concept of Assur virtual chain is presented in (Campos, 2004). This method allows to compute direct and inverse differential kinematics of serial and parallel manipulators in a unified way.

This article presents a kinematic model of automotive suspension, aiming to apply Davies' method together with the concept of Assur virtual chain. The proposed model is planar and it is composed by a chassis and two wheels, which are connected to the chassis by two McPherson type suspensions. In spite of being a quite simple model, it supplies information on characteristic parameters of the suspensions (camber, tread width, position of roll center and position of the center of gravity), which are not precisely represented in many models due to simplifications done in the kinematics of the suspension.

## 2. METHOD

Davies' method for kinematics is based on Kirchhoff Circulation Law. In this case, the method states that the algebraic sum of relative velocities of kinematic pairs along any closed kinematic chain is zero (Davies, 1981). The method can be described in ten steps: 1) Definition of kinematic chain, including Assur virtual chain; 2) Definition of the Coupling Graph; 3) Definition of the Motion Graph; 4) Definition of the Circuit Matrix; 5) Definition of normalized screws; 6) Definition of the unit motion matrix and the vector of motion magnitudes; 7) Definition of network unit motion matrix; 8) Assembly of the system of equations; 9) Solution of the system; and 10) Computing of the motions matrix.

### 2.1 Kinematic chain

Figure 1 shows the sketch of the model. The model has a chassis, two McPherson-type suspension and two wheels (left and right). The McPherson suspension is represented by two dampers (left and right) and two control arms (left and right).

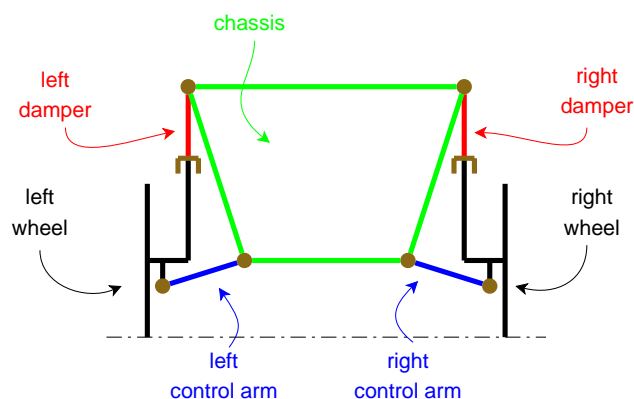


Figure 1. Sketch of the suspension mechanism.

Figure 2 shows the real kinematic chains including the Assur virtual chain. This virtual chain allows to control the chassis displacement. Links are identified by numbers. The fixed link is link number 1. Couplings are identified by lower cases roman letters.

### 2.2 Direct coupling graph

Figure 3 shows the direct coupling graph,  $G_C$ , corresponding to the kinematic chain showed in Figure 2. The coupling graph has 14 edges, ( $e = 14$ ), representing the couplings, and 11 vertex ( $v = 11$ ), representing the bodies. The edges are

oriented by arrows.

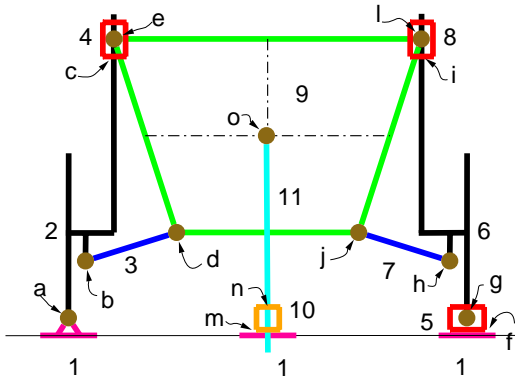


Figure 2. Kinematic chain.

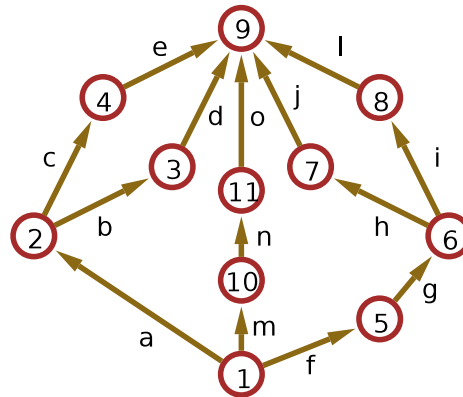


Figure 3. Coupling graph ( $G_C$ ) referring to Figure 2.

### 2.3 Motion graph

In the motion graph,  $G_M$ , each edge of  $G_C$  that represents a direct coupling of freedom  $f$  is replaced by  $f$  edges. Each edge of  $G_M$  represents a unit motion. The total number of edges of  $G_M$ ,  $F$ , is the gross degree of freedom of the kinematic chain. In this case,  $F = 14$ . Figure 4 shows the motion graph,  $G_M$ . The tree is formed by edges  $a - b - e - f - g - h - l - m - n - o$  and the chords are edges  $c, d, i,$  and  $j$ .

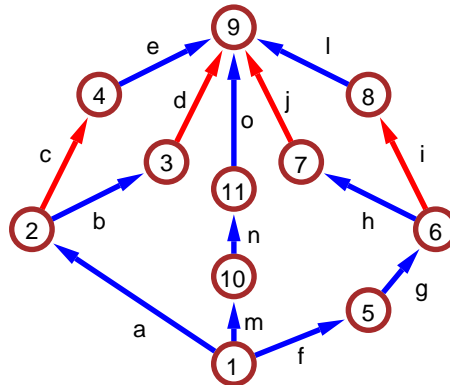


Figure 4. Motion graph  $G_M$ .

Figures 5 to 8 show each of the four circuits ( $l = 4$ ). Each circuit is identified and oriented according to its respective chord.

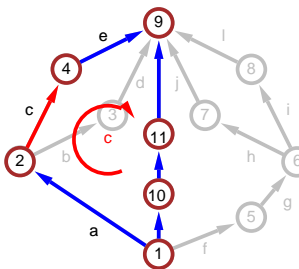


Figure 5. Circuit  $c$ .

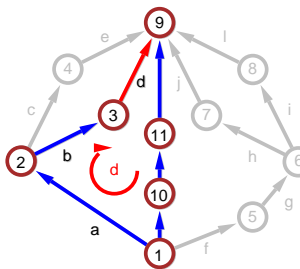


Figure 6. Circuit  $d$ .

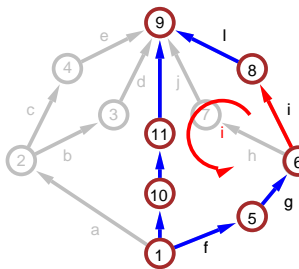


Figure 7. Circuit  $i$ .

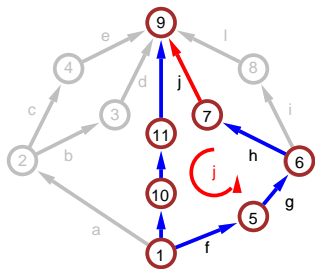


Figure 8. Circuit  $j$ .

### 2.4 Circuit matrix

The motion graph,  $G_M$ , has a corresponding circuit matrix,  $[B_M]_{l,F}$ . Each element  $b_{ij}$  is: 0 if circuit  $i$  does not include edge  $j$ ; +1 if the positive sense of circuit  $i$  is in the same direction as the positive sense of the edge  $j$ ; and -1 if

those positive sense are opposed (Davies, 2000).

$$[B_M]_{l,F} = [B]_{4,14} = \begin{bmatrix} 1 & 0 & 1 & 0 & 1 & 0 & 0 & 0 & 0 & 0 & 0 & -1 & -1 & -1 \\ 1 & 1 & 0 & 1 & 0 & 0 & 0 & 0 & 0 & 0 & 0 & -1 & -1 & -1 \\ 0 & 0 & 0 & 0 & 0 & 1 & 1 & 0 & 1 & 0 & 1 & -1 & -1 & -1 \\ 0 & 0 & 0 & 0 & 0 & 1 & 1 & 1 & 0 & 1 & 0 & -1 & -1 & -1 \end{bmatrix} \quad (4)$$

### 2.5 Definition of unit screws

Four reference frames has been defined in order to make more easy the definition of the screws. The frames are represented in Figure 9 and their position are defined in Table 1.

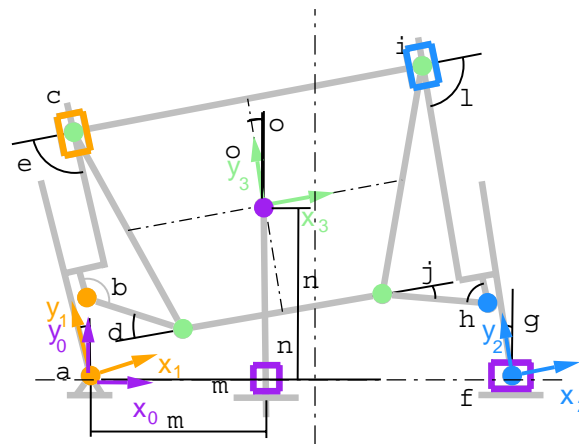


Figure 9. Global (0) and local(1, 2, and 3) reference systems.

Table 1. Position of local systems.

system	position			angle
	<i>x</i>	<i>y</i>	<i>z</i>	
1	0	0	0	$\theta_a$
2	$L_f$	0	0	$\theta_g$
3	$L_m$	$L_n$	0	$\theta_o$

First we define the unit screws locally and then we transform them to the global system. The reference system are:

- System 0: The global system, whose origin is on the contact point of the left wheel to the floor, and x-axis is horizontal.
- System 1: Placed on the contact point of the left wheel to the floor and parallel with the wheel plane.
- System 2: Placed on the contact point of the right wheel to the floor and parallel with the wheel plane.
- System 3: Placed on a point in the center of the chassis and oriented with its local horizontal and vertical directions.

In order to solve position kinematics, screws  $\$d$ ,  $\$e$ ,  $\$j$ , and  $\$i$  are also defined in system 3.

It is possible to compute the screws using expressions (3) and the data presented in Figure 10, Figure 11, and in Tables 2 and 3.

Transformation matrices transforms the velocity state from the local references to the global reference frame (Tsai, 1999):

$${}^i\hat{\$} = {}^i T_j \cdot {}^j\hat{\$} \quad (5)$$

where  ${}^i T_j$  is the transformation matrix of a screw in frame  $j$  to frame  $i$ , as follows

$${}^i T_j = \begin{bmatrix} {}^i R_j & \vdots & 0_{3 \times 3} \\ \cdots & \cdots & \cdots \\ {}^i W_j \cdot {}^i R_j & \vdots & {}^i R_j \end{bmatrix}, \quad \text{where} \quad {}^i W_j = \begin{bmatrix} 0 & -p_z & p_y \\ p_z & 0 & -p_x \\ -p_y & p_x & 0 \end{bmatrix}, \quad (6)$$

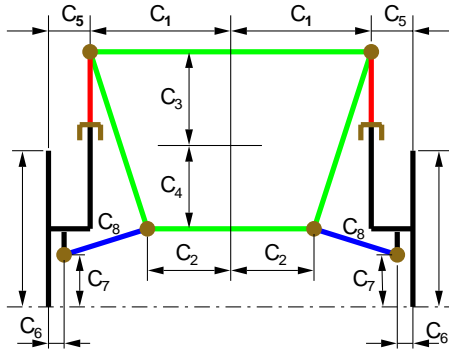


Figure 10. Body dimensions.

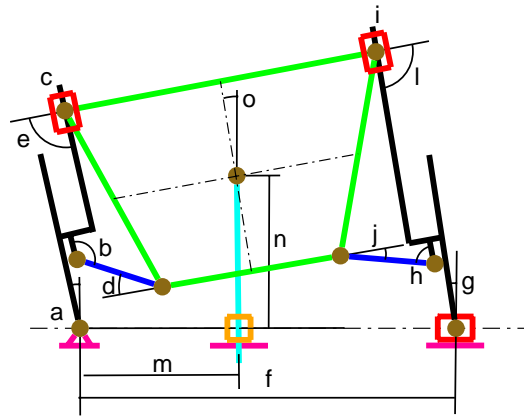


Figure 11. Magnitudes and their respective references.

Table 2. Identification and location of the couplings.

coupling	type	symbol	system	orientation			position		
				<i>x</i>	<i>y</i>	<i>z</i>	<i>x</i>	<i>y</i>	<i>z</i>
a	R	$\theta_a$	1	0	0	1	0	0	0
b	R	$\theta_b$	1	0	0	1	$C_6$	$C_7$	0
c	P	$L_c$	1	0	1	0	$C_5$	$r_p$	0
d	R	$\theta_d$	1	0	0	1	$C_6 + C_8 \cdot \sin \theta_b$	$C_7 + C_8 \cdot \cos \theta_b$	0
e	R	$\theta_e$	1	0	0	1	$C_5$	$r_p + L_c$	0
f	P	$L_f$	0	1	0	0	0	0	0
g	R	$\theta_g$	2	0	0	1	0	0	0
h	R	$\theta_h$	2	0	0	1	$-C_6$	$C_7$	0
i	P	$L_i$	2	0	1	0	$-C_5$	$r_p$	0
j	R	$\theta_j$	2	0	0	1	$-C_6 - C_8 \cdot \sin \theta_h$	$C_7 + C_8 \cdot \cos \theta_h$	0
l	R	$\theta_l$	2	0	0	1	$-C_5$	$r_p + L_i$	0
m	P	$L_m$	0	1	0	0	0	0	0
n	P	$L_n$	0	0	1	0	$L_m$	0	0
o	R	$\theta_o$	0	0	0	1	$L_m$	$L_n$	0
d	R		3	0	0	1	$-C_2$	$-C_4$	0
e	R		3	0	0	1	$-C_1$	$C_3$	0
j	R		3	0	0	1	$C_2$	$-C_4$	0
l	R		3	0	0	1	$C_1$	$C_3$	0

Table 3. Constants.

constant	value (mm)	description
C1	500	half-top width of the chassis
C2	300	half-bottom width of the chassis
C3	350	desistance between the reference point and the top of the chassis
C4	300	desistance between the reference point and the bottom of the chassis
C5	150	distance between damper and wheel
C6	50	knuckle length
C7	200	height of the lower pivot
C8	300	arm length
rp	300	tire radius

is a 3x3 skew-symmetric matrix representing the position of origin *j* expressed in the *i*th frame, and  ${}^iR_j$  is the rotation matrix from *j*th frame to *i*th frame as follows

$${}^0R_1 = \begin{bmatrix} \cos \theta_a & -\sin \theta_a & 0 \\ \sin \theta_a & \cos \theta_a & 0 \\ 0 & 0 & 1 \end{bmatrix} \quad {}^0R_2 = \begin{bmatrix} \cos \theta_g & -\sin \theta_g & 0 \\ \sin \theta_g & \cos \theta_g & 0 \\ 0 & 0 & 1 \end{bmatrix} \quad {}^0R_3 = \begin{bmatrix} \cos \theta_o & -\sin \theta_o & 0 \\ \sin \theta_o & \cos \theta_o & 0 \\ 0 & 0 & 1 \end{bmatrix}. \quad (7)$$

Table 1 shows the position vectors  ${}^iP_j$  of the three origins of the local frames.

## 2.6 Unit motion matrix and vector of magnitudes

The unit motion matrix,  $[\hat{M}_D]_{d,F}$ , has all the  $F$  unit screws of the kinematic chain, after the transformation to the global frame.

$$[\hat{M}_D]_{d,F} = [\hat{M}_D]_{3,14} = \left[ \hat{\$}_a \ \hat{\$}_b \ \hat{\$}_c \ \hat{\$}_d \ \hat{\$}_e \ \hat{\$}_f \ \hat{\$}_g \ \hat{\$}_h \ \hat{\$}_i \ \hat{\$}_j \ \hat{\$}_l \ \hat{\$}_m \ \hat{\$}_n \ \hat{\$}_o \right]. \quad (8)$$

The  $F$  magnitudes unknown are organized in the vector of magnitudes,  $\{\Phi\}_{F,1}$ , as

$$\Phi_{F,1} = \Phi_{14,1} = \{ w_a \ w_b \ v_c \ w_d \ w_e \ v_f \ w_g \ w_h \ v_i \ w_j \ w_l \ v_m \ v_n \ w_o \}^T. \quad (9)$$

## 2.7 Network unit motion matrix

The network unit motion matrix,  $[\hat{M}_N]_{dl,F}$ , represents the relation between the  $F$  unit screws, in  $[\hat{M}_D]_{d,F}$  (expression 8), with the  $l$  circuits, defined by the circuit matrix,  $[B_M]_{l,F}$  in expression (4). Each row of  $[B_M]_{l,F}$  informs the unit screws belonging to the circuit corresponding to that row. If the unit screw doesn't belong to that circuit, a null screw is inserted in the place. Taking account that this is a planar case, three coordinates ( $w_x, w_y$  e  $v_z$ ) are null. The dimension of the screw system is  $d = 3$ . So, for each circuit, there is  $d = 3$  rows in the network matrix, resulting in a  $d.l \times F$  or  $12 \times 14$  matrix, as follows.

$$\hat{M}_N = \begin{bmatrix} 1 & 0 & 0 & 0 & 1 & 0 & 0 & 0 & 0 & 0 & 0 & 0 & 0 & -1 \\ 0 & 0 & -\sin \theta_a & 0 & m_{1,5} & 0 & 0 & 0 & 0 & 0 & 0 & -1 & 0 & -L_n \\ 0 & 0 & \cos \theta_a & 0 & m_{2,5} & 0 & 0 & 0 & 0 & 0 & 0 & 0 & -1 & L_m \\ 1 & 1 & 0 & 1 & 0 & 0 & 0 & 0 & 0 & 0 & 0 & 0 & 0 & -1 \\ 0 & m_{5,2} & 0 & m_{5,4} & 0 & 0 & 0 & 0 & 0 & 0 & 0 & -1 & 0 & -L_n \\ 0 & m_{6,2} & 0 & m_{6,4} & 0 & 0 & 0 & 0 & 0 & 0 & 0 & 0 & -1 & L_m \\ 0 & 0 & 0 & 0 & 0 & 0 & 1 & 0 & 0 & 0 & 1 & 0 & 0 & -1 \\ 0 & 0 & 0 & 0 & 0 & 1 & 0 & 0 & -\sin \theta_g & 0 & m_{8,11} & -1 & 0 & -L_n \\ 0 & 0 & 0 & 0 & 0 & 0 & -L_f & 0 & \cos \theta_g & 0 & m_{9,11} & 0 & -1 & L_m \\ 0 & 0 & 0 & 0 & 0 & 0 & 1 & 1 & 0 & 1 & 0 & 0 & 0 & -1 \\ 0 & 0 & 0 & 0 & 0 & 1 & 0 & m_{11,8} & 0 & m_{11,10} & 0 & -1 & 0 & -L_n \\ 0 & 0 & 0 & 0 & 0 & 0 & -L_f & m_{12,8} & 0 & m_{12,10} & 0 & 0 & -1 & L_m \end{bmatrix} \quad (10)$$

where

$$\begin{aligned} m_{1,5} &= (r_p + L_c) \cdot \cos \theta_a + C_5 \cdot \sin \theta_a & m_{2,5} &= (r_p + L_c) \cdot \sin \theta_a - C_5 \cdot \cos \theta_a \\ m_{5,2} &= C_7 \cdot \cos \theta_a + C_6 \cdot \sin \theta_a & m_{5,4} &= (C_7 + C_8 \cdot \cos \theta_b) \cdot \cos \theta_a - (-C_6 - C_8 \cdot \sin \theta_b) \cdot \sin \theta_a \\ m_{6,2} &= C_7 \cdot \sin \theta_a - C_6 \cdot \cos \theta_a & m_{6,4} &= (C_7 + C_8 \cdot \cos \theta_b) \cdot \sin \theta_a + (-C_6 - C_8 \cdot \sin \theta_b) \cdot \cos \theta_a \\ m_{8,11} &= (r_p + L_i) \cdot \cos \theta_g - C_5 \cdot \sin \theta_g & m_{9,11} &= -L_f + (r_p + L_i) \cdot \sin \theta_g + C_5 \cdot \cos \theta_g \\ m_{11,8} &= C_7 \cdot \cos \theta_g - C_6 \cdot \sin \theta_g & m_{11,10} &= (C_7 + C_8 \cdot \cos \theta_h) \cdot \cos \theta_h - (C_6 + C_8 \cdot \sin \theta_h) \cdot \sin \theta_g \\ m_{12,8} &= -L_f + C_7 \cdot \sin \theta_g + C_6 \cdot \cos \theta_g & m_{12,10} &= -L_f + (C_7 + C_8 \cdot \cos \theta_h) \cdot \sin \theta_g + (C_6 + C_8 \cdot \sin \theta_h) \cdot \cos \theta_g \end{aligned} \quad (11)$$

## 2.8 Assembly of equation system

Davies' method states that the sum of the motion screws belonging to the same circuit is zero. For  $l$  circuits,

$$[\hat{M}_N]_{dl,F} \cdot \{\Phi\}_{F,1} = \{0\}_{dl,1}, \quad (12)$$

where  $[\hat{M}_N]_{dl,F}$  is the network unit motion matrix, defined in expression (10), and  $\{\Phi\}_{F,1}$  is the vector of motion magnitudes, defined in expression (9). For  $l$  independent circuits there are  $d.l$  equations imposing conditions on  $F$  unknown magnitudes. Where there are redundant equations it is because the kinematic chain is overconstrained. The cause might be that we have used a larger value for the dimension  $d$  than was necessary. This happens for example if we analyze a planar kinematic chain using  $d = 6$  (Davies, 2000). After removing redundant rows of the system, the remaining  $m$  rows form the final system:

$$[\hat{M}_N]_{m,F} \cdot \{\Phi\}_{F,1} = \{0\}_{m,1}. \quad (13)$$

The nett degree of freedom of the coupling network is (Davies, 2006):

$$F_N = F - m. \quad (14)$$

In this case,  $m = d.l = 12$ , and  $F_N = F - m = 14 - 12 = 2$  primary variables are necessary to describe the motion.

## 2.9 Solution of the system

To obtain the solution for (13), it is necessary to identify a suitable set of  $F_N$  primary variables from among the  $F$  unknowns in  $\Phi$ . Once the set has been identified, the system (13) is partitioned in two sets, as follows

$$\begin{bmatrix} [\hat{M}_{NS}]_{m,m} & : & [\hat{M}_{NP}]_{m,F_N} \end{bmatrix} \begin{Bmatrix} \{\Phi_S\}_{m,1} \\ \dots \\ \{\Phi_P\}_{F_N,1} \end{Bmatrix} = \{0\}_{m,1} \quad (15)$$

where  $\{\Phi_P\}_{F_N,1}$  is the vector of primary magnitudes,  $\{\Phi_S\}_{m,1}$  is the vector of secondary magnitudes,  $[\hat{M}_{NP}]_{m,F_N}$  is the network primary matrix, and  $[\hat{M}_{NS}]_{m,m}$  is the network secondary matrix.

In this case, the vector of primary magnitudes is

$$\psi_P = \{ v_n \quad w_o \}^T \quad (16)$$

and the vector of secondary magnitudes is

$$\{\psi_S\}_{12,1} = \{ w_a \quad w_b \quad v_c \quad w_d \quad w_e \quad v_f \quad w_g \quad w_h \quad v_i \quad w_j \quad w_l \quad v_m \}^T. \quad (17)$$

The network matrices  $M_{NS}$  and  $M_{NP}$  are obtained by selecting the corresponding columns.

The system (13) is solved, resulting

$$\{\Phi_S\}_{m,1} = - [\hat{M}_{NS}]_{m,m}^{-1} [\hat{M}_{NP}]_{m,F_N} \{\Phi_P\}_{F_N,1}. \quad (18)$$

The solution results in the secondary variables  $\{\Phi_S\}_{m,1}$  expressed in terms of  $F_N$  primary variables  $\{\Phi_P\}_{F_N,1}$ .

## 2.10 Computing the motion matrix

After the reconstruction of the vector of motion magnitudes  $\Phi_{F,1}$ , (9), the motion matrix  $[M_D]_{d,F}$  can be created by multiplying each column of  $[\hat{M}_D]_{d,F}$  by the corresponding element of  $\Phi_{F,1}$ , resulting

$$[M_D]_{d,F} = [\hat{M}_D]_{d,F} \cdot \text{diag}(\Phi), \quad (19)$$

where  $\text{diag}(\Phi)$  is a diagonal matrix with the magnitudes as the diagonal elements.

## 3. RESULTS

To illustrate the results, two cases of motion are presented:

**Case 1:** A vertical motion (heave) is applied to the chassis, with  $L_n$  varying from 400 mm to 600 mm. The other primary variables are:  $\theta_o = 0$ ,  $\dot{L}_n = 1$  m/s, and  $\dot{\theta}_o = 0$  rad/s.

**Case 2:** A roll movement is applied to the chassis, with  $L_n = 500$  mm,  $\theta_o$  varying from  $-10$  to  $+10$  degrees,  $\dot{L}_n = 0$  m/s, and  $\dot{\theta}_o = 1$  rad/s.

### 3.1 Finding relative velocity between unconnected bodies

To find the motion between two indirectly coupled bodies  $i$  and  $j$ , it is necessary to select any path of  $G_M$  in Figure 4. The velocity of the chassis in the reference frame, for example, is obtained by one of the following sums:

$$\begin{aligned} & \$_a + \$_b + \$_d, \\ & \$_a + \$_c + \$_e, \\ & \$_m + \$_n + \$_o, \\ & \$_f + \$_g + \$_h + \$_j \text{ ou} \\ & \$_f + \$_g + \$_i + \$_l \end{aligned} \quad (20)$$

The magnitude of the screw represents the relative motion between the connected bodies. Figures 12 to 15 shows angular and linear relative velocity of the bodies for 50 instant positions of the displacement. Refer to Figure 11 to identify the components.

### 3.2 Relations between magnitudes

The resulting magnitudes  $\Phi_{F,1}$  supply the geometry of the suspension: magnitudes  $a$  and  $g$  describe camber angle displacement in both wheels. Magnitude  $f$  describes tread width,  $n$  describes chassis height, and  $o$  describes chassis roll. For Case 1, chassis height x tread width and chassis height x camber are presented in Figures 16 and 17, respectively. For Case 2, roll angle x tread width and roll angle x camber are presented in Figures 18 and 19, respectively.

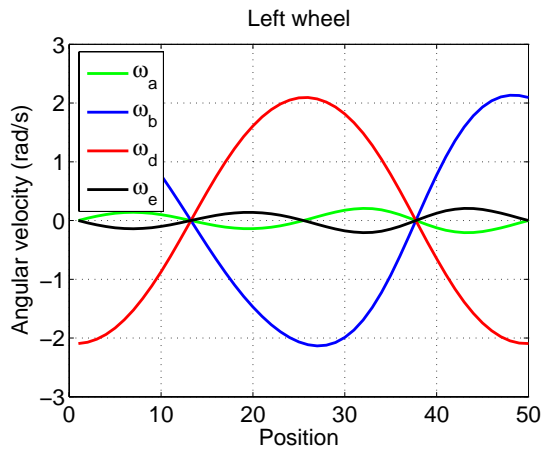


Figure 12. Angular velocity of left wheel couplings.

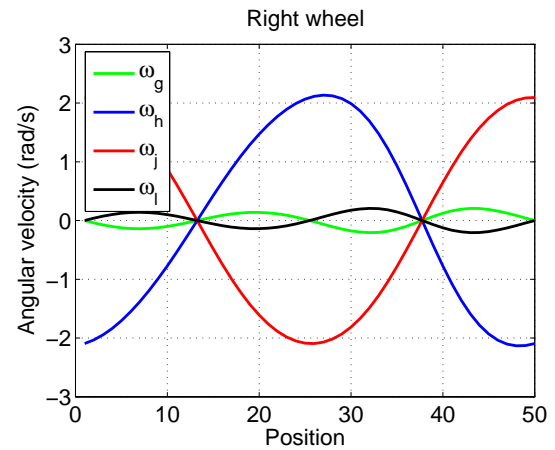


Figure 13. Angular velocity of right wheel couplings.

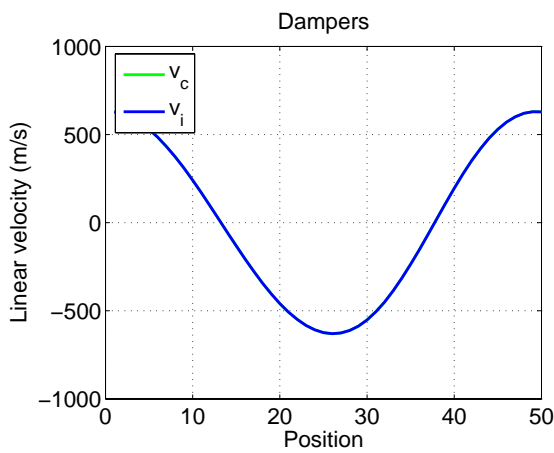


Figure 14. Linear velocity of dampers.

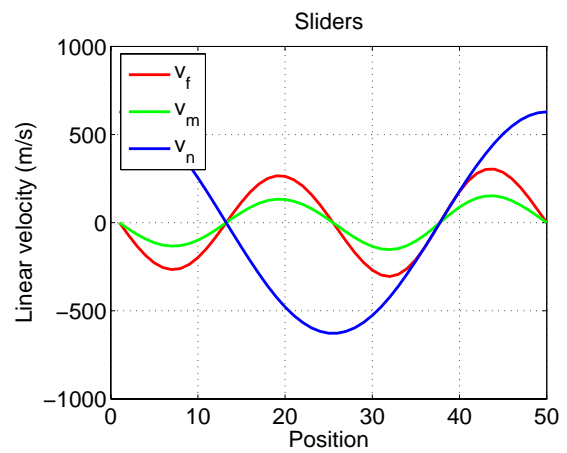


Figure 15. Linear velocity of sliders  $f$ ,  $m$ , and  $n$ .

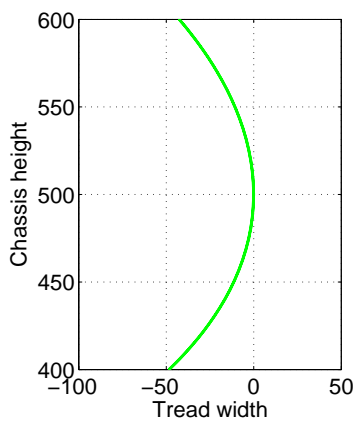


Figure 16. Chassis height x tread width.

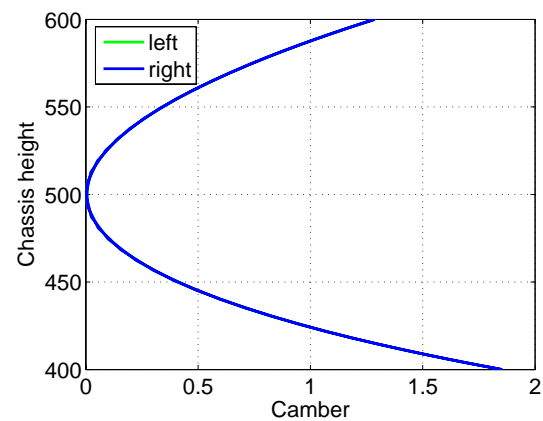


Figure 17. Chassis height x camber.

### 3.3 Getting the position of interest points

Position of roll center, can be achieved taking account the screw representing the chassis motion ( $\$_o$ ):

$$\$_o = \begin{Bmatrix} w_z \\ v_x \\ v_y \end{Bmatrix} = \begin{Bmatrix} 1 \\ p_{oy} \\ -p_{ox} \end{Bmatrix} \cdot w_o \quad (21)$$

Thus,  $p_{ox}$  coordinate is the negative of the third normalized screw component and  $p_{oy}$  coordinate is the second normalized screw component. Figure 20 shows roll center position for Case 2.

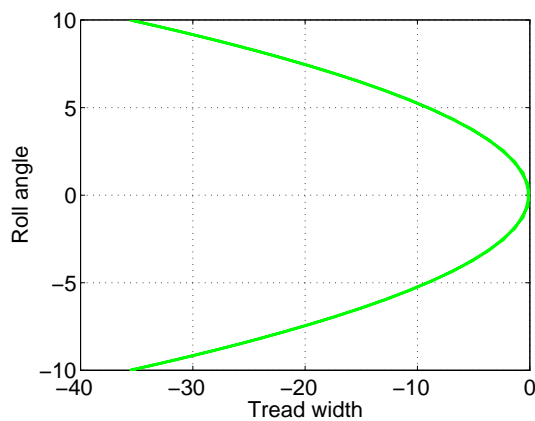


Figure 18. Roll angle x tread width.

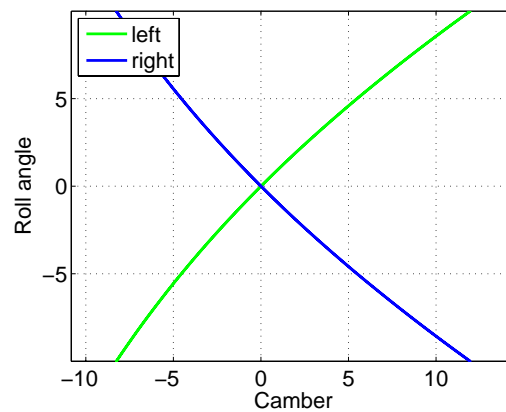


Figure 19. Roll angle x camber.

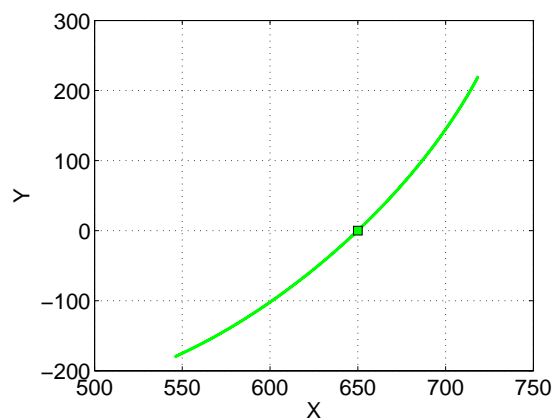


Figure 20. Roll center position.

#### 4. DISCUSSION

A kinematic model of suspension based on Davies method using Assur virtual chain has been presented in this article. The model produces displacements and relative motions between any pair of selected bodies in the kinematic chain. The presented cases show the influence of chassis height and roll angle in camber and tread width. However, it is possible to compute displacement and motion between any pairs of bodies of the kinematic chain. To represent other type of suspension, is enough to change the graphs,  $G_C$  and  $G_M$ , the circuit matrix,  $[B_M]_{l,F}$ , and the position and orientation vectors of each couple. The combination of Davies' method and Assur virtual chains is a powerful tool to automatize the kinematics analysis. The next stage of the research is to extend the model for static analysis.

#### 5. ACKNOWLEDGEMENTS

This work was supported by 'Coordenação de Aperfeiçoamento de Pessoal de Nível Superior' (CAPES), Brazil.

#### 6. REFERENCES

- Campos, A. (2004). *Cinemática diferencial de manipuladores empregando cadeias virtuais*. Tese, Universidade Federal de Santa Catarina, Florianópolis.
- Campos, A., Guenther, R., and Martins, D. (2005). Differential kinematics of serial manipulators using virtual chains. *Journal of the Brazilian Society of Mechanical Science and Engineering*, XXVII(4):345–356.
- Campos, A., Martins, D., and Guenther, R. (2003). A unified approach to differential kinematics of nonredundant manipulators. In *The 11th International Conference on Advanced Robotics*, pages 1837–1842.
- Chang, K.-H. and Joo, S.-H. (2005). CAD-Based Design Optimization for Vehicle Performance. In *6th World Congresses of Structural and Multidisciplinary Optimization*, page 10.
- Chen, K. and Beale, D. G. (2003). Base dynamic parameter estimation of a MacPherson suspension mechanism. *Vehicle System Dynamics*, 39(3):227–244.
- Costa Neto, A. (1992). *Application of multibody system (MBS) techniques to automotive vehicle chassis simulation for*

- motion control studies*. PhD thesis, University of Warwick, Warwick.
- Davidson, J. K. and Hunt, K. H. (2004). *Robots and Screw Theory: Applications of Kinematics and Statics to Robotics*. Oxford University Press, New York.
- Davies, T. H. (1981). Kirchhoff's circulation law applied to multi-loop kinematic chains. *Mechanism and Machine Theory*, 16(3):171–183.
- Davies, T. H. (1995a). Circuit actions attributable to active couplings. *Mechanism and Machine Theory*, 30(7):1001–1012.
- Davies, T. H. (1995b). Couplings, coupling networks and their graphs. *Mechanism and Machine Theory*, 30(7):991–1000.
- Davies, T. H. (2000). The 1887 Committee Meets Again. Subject: freedom and constraint. In *University of Cambridge*, page 56, Cambridge. Proceedings of A Symposium Commemorating the Legacy, Works, and Life of Sir Robert Stawell Ball upon the 100th Anniversary of "A Treatise on the Theory of Screws", Cambridge University Press.
- Davies, T. H. (2006). Freedom and constraint in coupling networks. In *Journal of Mechanical Engineering Science*, volume 220, pages 989–1010.
- Dixon, J. C. (1996). *Tires, Suspension, and Handling*. SAE International, Warrendale, 2 edition.
- Fayet, M. (2000). Wrench-twist duality in over-constrained mechanisms. In *Anais do evento A Symposium Commemorating the Legacy, Works, and Life of Sir Robert Stawell Ball*, page 21. University of Cambridge. Digite o texto aqui.
- Gallardo, J., Rico, J., Frisoli, A., Checcacci, D., and Bergamasco, M. (2003). Dynamics of parallel manipulators by means of screw theory. *Mechanism and Machine Theory*, 38:1113–1131.
- Gillespie, T. D. (1992). *Fundamentals of Vehicle Dynamics*. SAE International, Warrendale.
- Hac, A. (2002). Rollover Stability Index Including Effects of Suspension Design. In *SAE 2002 World Congress*, number 2002-01-0965, page 11. SAE International.
- Hunt, K. H. (1978). *Kinematic geometry of mechanisms*. Clarendon Press.
- Mántaras, D. A., Luque, P., and Vera, C. (2004). Development and validation of a three-dimensional kinematic model for the McPherson steering and suspension mechanisms. *Mechanism and Machine Theory*, 39:603–619.
- Martins, D. (2002). *Análise cinemática hierárquica de robôs manipuladores*. Tese, Universidade Federal de Santa Catarina.
- Perna, G., Poian, M., and Poloni, C. (2000). Multi Objective optimization of a car vehicle coupling FRONTIER and MDI-ADAMS. In *15th European ADAMS Users' Conference*, page 19. MSC Software Corporation.
- Reimpell, J., Stoll, H., and Betzler, J. W. (2001). *The Automotive Chassis: Engineering Principles*. Society of Automotive Engineers.
- Rill, G. (2003). Vehicle Dynamics. Lecture notes, Fachhochschule Regensburg.
- Shabana, A. A. (2003). *Dynamics of Multibody Systems*. Cambridge University Press, 2 edition.
- Tsai, L.-W. (1998). The Jacobian analysis of a parallel manipulator using the theory of reciprocal screws. Technical Report T.R. 98-34, Institute for Systems Research, Maryland.
- Tsai, L.-W. (1999). *Robot Analysis - The Mechanics of Serial and Parallel Manipulators*. John Wiley & Sons, Inc., New York.
- Tsai, L.-W. (2000). *Mechanism Design: Enumeration of Kinematic Structures According to Function*. CRC Press, London.
- Valdiero, A. C., Campos, A., Guenther, R., and Matrins, D. (2001). Cálculo e Análise do Jacobiano de um manipulador paralelo de 3 graus de liberdade baseado na teoria dos helicóides. In *IX Congresso Brasileiro de Engenharia Mecânica*, page 10.

## 7. RESPONSIBILITY NOTICE

The authors are the only responsible for the printed material included in this paper